Received: 26 March 2018 | Revised: 4 December 2018 | Accepted: 7 December 2018

DOI: 10.1111/exd.13862

ORIGINAL ARTICLE

WILEY Experimental Dermatology

UV-B-activated B16 melanoma cells or HaCaT keratinocytes accelerate signaling pathways associated with melanogenesis via ANGPTL 2 induction, an activity antagonized by Chrysanthemum extract

Gaku Satou[1] | Daisuke Maji[1] | Takayuki Isamoto[1] | Yuichi Oike[2] | Motoyoshi Endo[2,3]

[1]Saishunkan Pharmaceutical Co. Ltd, Kumamoto, Japan

[2]Department of Molecular Genetics, Graduate School of Medical Sciences, Kumamoto University, Kumamoto, Japan

[3]Department of Molecular Biology, University of Occupational and Environmental Health, Japan, Fukuoka, Japan

Correspondence
Motoyoshi Endo, Department of Molecular Biology, University of Occupational and Environmental Health, Japan, Yahatanishi-ku, Kitakyushu, Japan.
Email: mendo@med.uoeh-u.ac.jp

Funding information
Saishunkan Pharmaceutical Co., Ltd

Abstract

Sunburn causes inflammation, which increases melanin production in skin and causes hyperpigmentation. Angiopoietin-like protein (ANGPTL) 2 is an inflammatory mediator induced in sun-exposed skin areas. However, whether ANGPTL2 functions in melanin production remains unclear. To assess this possibility, we overexpressed *Angptl2 in* the melanoma line B16 and in the keratinocyte line HaCaT. Relative to controls, *Angptl2*-expressing B16 cells produced higher melanin levels via tyrosinase induction. Accordingly, *Angptl2*-expressing HaCaT cells secreted relatively high levels of both endothelin-1 (ET-1) and α-melanocyte-stimulating hormone (α-MSH). Moreover, treatment with an extract from *Chrysanthemum indicum* × *Erigeron annuus* (CE) suppressed ANGPTL2 expression and repressed tyrosinase induction in melanocytes and of α-MSH and ET-1 in keratinocytes. Our data suggest that ANGPTL2 expression in keratinocytes and melanin-producing cells accelerates pigment production and that treatment of skin with a CE extract could prevent melanin accumulation.

KEYWORDS
angiopoietin-like protein 2, Chrysanthemum, melanin

1 | INTRODUCTION

Skin hyperpigmentation, which can be caused by either sun exposure, some medications, skin inflammation or hormonal changes, is a significant concern, particularly for women.[1] Therefore, effective treatments to prevent this condition are desirable. Ultraviolet B (UV-B) irradiation is the primary cause of hyperpigmentation due to excessive melanin production.[2,3] UV-B-exposed keratinocytes produce cytokines and upregulate secretion of endothelin-1 (ET-1) and α-melanocyte-stimulating hormone (α-MSH), both of which promote induction of tyrosinase, the rate-limiting enzyme catalysing melanin synthesis,[2,3] in melanocytes. Therefore, inhibition of ET-1 or α-MSH secretion by keratinocytes and/or tyrosinase induction in melanocytes could prevent melanin production in the latter following UV-B exposure.[4]

Angiopoietin-like protein 2 (ANGPTL2) is a secreted protein that induces inflammation in various cell types via autocrine or paracrine signals.[5] ANGPTL2 upregulation exacerbates various diseases, such as cardiovascular disease, diabetes or cancer by enhancing inflammation.[6–10] We previously reported that ANGPTL2 expression was higher in UV-exposed areas of human skin than in unexposed areas.[11] However, as yet, no reports link ANGPTL2 expression with melanin production in skin tissue.

Many traditional medicines derived from natural products have been used to block melanin synthesis.[12,13] In particular, a retrospective search for cosmetic agents based on traditional Chinese medicines made from natural products has recently been reported.[14] Novel products to inhibit melanin production based on these approaches could have cosmetic applications.

Here, we evaluate ANGPTL2 function in melanin production. We report that UV-B irradiation induced ANGPTL2 in both keratinocytes and melanoma cells. ANGPTL2 overexpression in keratinocytes induced α-MSH and ET-1 production by those cells, while ANGPTL2 overexpression in melanoma cells induced tyrosinase. We also found that treatment of keratinocytes or melanoma cells with an extract from "*Chrysanthemum indicum* × *Erigeron annuus*" (CE) inhibited ANGPTL2 expression in both cell types. These results suggest a new strategy to block ANGPTL2 expression and melanin accumulation following sun exposure.

2 | MATERIALS AND METHODS

2.1 | Cell culture

The mouse skin melanoma line B16 and the human pancreatic cancer line HPAC were cultured in Dulbecco's modified Eagle's medium (Sigma-Aldrich, St Louis, MO, USA) supplemented with 10% foetal bovine serum, 100 units/mL penicillin (Wako, Osaka, Japan), and 100 μg/mL streptomycin (Wako) in a humidified atmosphere of 95% air with 5% CO_2 at 37°C. The human skin keratinocyte cell line HaCaT was cultured in Dulbecco's modified Eagle's medium supplemented with 5% foetal bovine serum, 100 units/mL penicillin and 100 μg/mL streptomycin in a humidified atmosphere of 95% air with 5% CO_2 at 37°C. Transfection of either cell type with an *Angptl2* expression vector (pcDNA3.1 harbouring either mouse or human *Angptl2)* or control vector was carried out using Lipofectamine (2000) (ThermoFisher, Waltham, MA, USA), according to the manufacturer's protocol. Stable *Angptl2* transfectants were selected in G418 and analysed by ELISA (IBL, Fujioka, Gunma, Japan). Positive clones were maintained in culture with 1000 μg/mL G418 (Sigma-Aldrich).

2.2 | Quantification of melanin content in vitro

Melanin content of cultured cells was measured as described.[15,16] Briefly, medium was replaced, cells were cultured 48 hours and cells were then homogenized in 3N NaOH (Wako). Melanin content of homogenates was determined by measuring absorbance at 405 nm using a plate reader (ARVO™ X3; PerkinElmer, Waltham, MA, USA).

2.3 | Tyrosinase activity assay

Tyrosinase activity was assayed as described.[17] Briefly, cells were washed with phosphate-buffered saline and homogenized in 20 mmol/L Tris/HCl (pH 7.5) containing 0.1% Triton X-100 (Sigma-Aldrich). Tyrosinase activity assayed as oxidation of L-DOPA to DOPAchrome was monitored as follows. Cell extracts (100 μg/mL) were mixed with 100 μL freshly prepared substrate solution (0.1% L-DOPA in phosphate-buffered saline) and incubated 20 minutes at 37°C. DOPAchrome production was monitored by measuring absorbance at 490 nm using a plate reader (ARVO™ X3).

2.4 | Real-time RT-PCR analysis

Total RNA was extracted from cells using TRIZOL reagent (Thermo Fisher Scientific, Waltham, MA, USA), according to the manufacturer's protocol. Samples (1.0 μg RNA) were reverse-transcribed using PrimeScript™ RT Master Mix (TaKaRa, Kusatsu, Japan). Synthesized cDNA was subjected to real-time RT-PCR (CFX Connect™; Bio-Rad, Hercules, CA, USA) using SYBR Green Supermix (Bio-Rad), and results were analysed with CFX Manager Software (Bio-Rad). For transcript normalization, beta-actin cDNA served as an internal standard. Primers were designed using the Primer3 website. Primers used were (forward and reverse, respectively): mouse *Angptl2*, CAGAAGGGAGGATGGTGGTA and CAGTAGACCCCGTCCTGGTA; human *Angptl2*, ACCGA GTGCATAAGCAGGAG and AGCTTCACCTCGCTCACAAT; mouse β-*actin* (for an internal control), GACGGCCAGGTCATCACTAT and CT TCTGCATCCTGTCAGCAA; human *18s rRNA* (for an internal control), CCGCAGCTAGGAATAATGGA and CCCTCTTAATCATGGCCTCA; mouse *Tyr*, GCACTGGTGGGAGCTGTTAT and CAGCAA GCTGTGGTAGTCGT; human *Pomc*, CCCTACAGGATGGAGCACTT and TTGATGATGGCGTTTTTGAA; human *Edn1*, ACCATCTT CACTGGCTTCCA and GTCAGAAACTCCACCCCTGT; mouse *Mitf*, AACTGCAGCCAGGAACTTGT and TCTTCCTGGGGATGCTGTAG; mouse *Trp1*, TGGCCAGGTCAGGAGTTTAC and TCAGTGA GGAGAGGCTGGTT; and mouse *Trp2*, CTTCCTAACCGCAGAGCAAC and AGACGAAAGCTCCCAGGATT.

For quantitative real-time PCR analysis of mouse and human *Angptl2*, the amplification product was quantified using standard curves obtained from 10^4 to 10^7 copies of plasmid template. cDNA was amplified for 30 cycles, and values were normalized to β-actin levels. We utilized β-*actin* primers based on identical human and mouse sequences: GAGACCTTCAACACCCCAGCCAT and TACTCCTGCTTGCTGATCCACAT.

2.5 | Immunoblot analysis

Cells were homogenized in lysis buffer (10 mmol/L NaF, 1 mmol/L Na_3VO_4, 1 mmol/L EDTA, 300 mmol/L NaCl, 50 mmol/L Tris-HCl, 1% Triton X-100, pH 7.5). Extracts derived from supernatants (20 μg protein/lane) were subjected to SDS-polyacrylamide gel electrophoresis, and proteins were electrotransferred to nitrocellulose membranes. Immunodetection was performed using an Amersham ECL kit (GE Healthcare, Chicago, IL, USA) according to the manufacturer's protocol. Polyclonal rabbit antibodies against NFATc2 (M-300: diluted 1000-fold) and monoclonal mouse antibodies against Hsc70 (B-6: diluted 1000-fold) were obtained from Santa Cruz (Dallas, TX, USA).

2.6 | Quantification of ANGPTL2, α-MSH and ET-1 protein by ELISA

B16 and HaCaT cells were grown to 90% confluency on 6-well plates and cultured for 48 hours after replacement of medium. ANGPTL2

protein levels in culture media were measured by ELISA using an ANGPTL2 Assay Kit (IBL), according to the manufacturer's instructions. Respective α-MSH and ET-1 protein levels in HaCaT cell culture medium were measured by ELISA using an α-MSH Assay Kit (CUSABIO, Hebei, China) and an ET-1 Assay Kit (Abcam, PLC, Cambridge, UK), according to manufacturers' instructions.

2.7 | Cell viability analysis

Cells were counted using a Cell Counting Kit-8 (CCK8; Dojindo Laboratories, Kumamoto, Japan), according to the manufacturer's instructions. Briefly, B16 cells were plated in 96-well plates at 2000 cells/well with various concentration of Chrysanthemum Extract (CE) in 200 μL of culture medium. After 24 hours, CCK8 solution was added to each, and plates were incubated 1 hour at 37°C. Absorbance at 450 nm was determined using a microplate reader (ARVO™ X3).

2.8 | UV-B treatment

Cells were exposed to UV-B irradiation (30 mJ) using a UVB lamp (peak emission at 312 nm; TL20W/12RS lamp, Dermaray 200; Muranaka Medical Instruments, Osaka, Japan). UV energy was monitored with a radiometer sensor (UVX-31; TGK, Tokyo, Japan), and cells were analysed 24 hours later.

2.9 | IBMX treatment

B16 cells were grown to 90% confluency on 6-well plates. The medium was then replaced, and cells were cultured 24 hours with 3-isobutyl-1-methylxanthine (IBMX) and/or CE prior to analysis.

2.10 | Measurement of mushroom tyrosinase activity

For in vitro assays, 50 μL mushroom tyrosinase (50 U/mL; Sigma-Aldrich (EC 232-653-4)) plus 100 μL of 1 mmol/L Kojic acid or CE solution were placed in wells of a 96-well plate and incubated 10 minutes at room temperature. Then, 100 μL of the substrate 0.1% L-DOPA (3,4- dihydroxyphenylalanine) (Wako) was added, and the plate was further incubated at 25°C for 20 minutes. Subsequently, absorbance of DOPAchrome (the product) was measured at 490 nm using a microplate reader (ARVO™ X3). Kojic acid served as a positive control for tyrosinase inhibition and phosphate buffer as the negative control.

2.11 | Screening of natural product inhibitors of ANGPTL2 expression

HPAC cells, which express high levels of ANGPTL2, were used for inhibitor screening. 10 μL each of 97 traditional Chinese medicines (see Table 1) derived from natural products (0.1 mg/mL solvated with 1,3-butanediol) was dissolved in 1 mL Dulbecco's modified Eagle's medium without foetal bovine serum and then added to confluent HPAC cells plated on 24-well plates. ANGPTL2 protein levels in culture media at 24 hours later were then measured by ELISA (IBL).

2.12 | *Angptl2* knockdown

B16 cells were reseeded on 6-well plates and incubated with *Angptl2* siRNA (customized and designed by SIGMA-ALDRICH) using RNAi MAX transfection reagent (ThermoFisher), according to the manufacturer's instructions. A scrambled siRNA (BIONEER (SN-1001)) served as a negative control.

3 | RESULTS

3.1 | Melanin content of melanoma cells increases following *Angptl2* overexpression

We previously reported induction of ANGPTL2 mRNA in sun-exposed human skin tissue.[11] Therefore, we asked whether ultraviolet (UV)-B induces ANGPTL2 in melanoma cells using the mouse melanoma line B16. UV-B-irradiated B16 cells showed increased *Angptl2* mRNA expression relative to non-treated controls (Figure 1A). To determine whether ANGPTL2 expression promotes melanin production in melanoma cells, we established mouse *Angptl2*-overexpressing B16 cells (Figure 1B) and found that in the absence of radiation, they produced greater levels of melanin than did mock-transfected B16 control cells (Figure 1C). In addition, levels of tyrosinase mRNA, which encodes the enzyme catalysing melanin production, were higher in *Angptl2*-overexpressing relative to control B16 cells (Figure 1D), strongly suggesting that ANGPTL2 expression in melanoma cells promotes melanin production. We then assessed transcript levels of *Mitf*, a key transcriptional regulator of the *Tyr* gene, in *Angptl2*-overexpressing and control B16 cells but observed no differences (Figure 1E). Expression of tyrosinase-related protein *(Trp)-1*, and *Trp-2* mRNA, both downstream of *Mitf*, was also comparable in *Angptl2*-overexpressing and control B16 cells (Figure 1F,G). We conclude that tyrosinase induction by ANGPTL2 in B16 cells is not due to *Mitf* induction.

3.2 | α-MSH and ET-1 expression increases in an *Angptl2*-overexpressing keratinocyte line

Following UV-B irradiation or inflammation, keratinocytes increase secretion of α-MSH and ET-1, which in turn activates melanin production by melanocytes non-cell autonomously.[18,19] Given our observation that ANGPTL2 is induced in sun-exposed skin,[11] we hypothesized that ANGPTL2 expressed in keratinocytes might induce α-MSH and/or ET-1 secretion by those cells. To assess this possibility, we first confirmed that human keratinocyte HaCaT cells upregulated ANGPTL2 mRNA expression following UV-B radiation (Figure 1H). We then generated *Angptl2*-overexpressing HaCaT cells (Figure 1I) and assayed α-MSH and ET-1 protein levels in culture medium. Over a 24-hour period, levels of α-MSH and ET-1 proteins in the medium of

TABLE 1 A list of 97 traditional Chinese medicines derived from natural products (left) and evaluated for effects on ANGPTL2 secretion by HPAC cells

No.	Scientific name	Relative ANGPTL2 protein level	No.	Scientific name	Relative ANGPTL2 protein level
1	*Houttuynia cordata*	1.0034	51	*Moringa oleifera* Lam.	0.8372
2	*Azadirachta indica*	0.9765	52	*Spinacia oleracea*	0.6771
3	*Cynara scolymus*	1.0854	53	*Daucus carota* subsp. *Sativus*	0.9008
4	*Litchi chinensis*	0.1029	54	*Cucurbita moschata*	0.9011
5	*Scutellaria baicalensis*	0.9486	55	*Ipomoea batatas*	0.8055
6	*Aloe vera*	0.6332	56	*Arctium lappa* L.	0.9800
7	*Ginkgo biloba*	0.6124	57	*Brassica rapa* var. *perviridis*	0.7287
8	*Tamarindus indica L.*	0.1483	58	*Zea mays*	0.8109
9	*Camellia sinensis*	0.3638	59	*Citrus junos*	0.8895
10	*Curcuma longa*	0.9471	60	*Oryza sativa* Linne (sprouted brown rice)	0.8239
11	*Alpinia zerumbet*	0.7697	61	*Oryza sativa* Linne (Gramineae)	0.9161
12	*Engelhardia roxburghiana*	0.7946	62	*Zingiber officinale*	0.7741
13	*Panax ginseng*	0.6269	63	*Theobroma cacao*	0.9639
14	*Psidium guajava* L.	0.0980	64	*Actinidia deliciosa*	0.9260
15	*Averrhoa carambola*	0.3176	65	*Zingiber officinale* var. *rubrum*	0.7864
16	*Rubus suavissimus*	0.4003	66	*Juglans*	0.3954
17	*Ampelopsis glandulosa* var. *heterophylla*	0.5095	67	*Allium tuberosum*	0.9602
18	*Nelumbo nucifera*	1.1394	68	*Cistanche Tubulosa* (Schenk) R. Wight	0.3056
19	*Piper longum*	0.8013	69	*Oryza sativa* subsp. *Japonica*	0.7454
20	*Tilia miqueliana*	0.3317	70	*Tremella fuciformis*	1.0520
21	*Acer maximowiczianum*	0.4827	71	*Vaccinium vitis-idaea* L.	0.7922
22	*Smallanthus sonchifolius*	0.6359	72	*Fragaria × ananassa Duch*	0.7696
23	*Melissa officinalis*	0.9806	73	*Laminaria japonica*	0.6576
24	*Rosa gallica officinalis*	0.6288	74	*Cerasus* Mill.	0.8195
25	*Astragalus complanatus* R.Br. Ex Bunge.	0.6511	75	*Coprinus comatus*	0.6884
26	*Actinidia polygama*	0.8826	76	*Citrus junos*(seed)	0.9673
27	*Allium sativum*	0.8028	77	*Petasites japonicus*	0.8728
28	*Eutrema japonicum*	0.6877	78	*Coffea arabica*	1.0377
29	*Centella asiatica*	0.7242	79	*Oenothera tetraptera*	0.0584
30	*Tambourissa trichophylla*	0.2482	80	*Fagopyrum esculentum*	1.0124
31	*Lepidium meyenii*	0.7145	81	*Perilla frutescens* var. *crispa*	1.0466
32	*Vaccinium myrtillus*	0.3299	82	*Oryza sativa* Linne (whole rice)	1.0254
33	*Sparassis crispa*	0.6482	83	*Brassica oleracea*	1.0336
34	*Amorphophallus konjac*	0.9113	84	*Chrysanthemum indicum × Erigeron annuus* (water extract)	0.2028
35	*Phyllanthus emblica*	0.4730	85	*Chrysanthemum indicum × Erigeron annuus* (ethanol extract)	0.1967
36	*Garcinia cambogia*	0.9117	86	*Glycine max* (Black Soya bean)	0.5357
37	*Punica granatum*	0.5020	87	*Morus* (water extract)	0.9783
38	*Vitis vinifera* L.	0.0272	88	*Juncus effusus* L. var. *decipens* Buchen (water extract)	1.0674
39	*Boswellia serrata*	0.8900	89	*Bletilla striata* Reichb. Fil	1.0763

(Continues)

TABLE 1 (Continued)

No.	Scientific name	Relative ANGPTL2 protein level	No.	Scientific name	Relative ANGPTL2 protein level
40	*Triticum aestivum*	0.9694	90	*Eriobotrya japonica*	0.3735
41	*Cocos nucifera* L.	0.6474	91	*Gentiana lutea* L	1.0083
42	*Phaeophyceae*	0.6508	92	*Ficus carica*	0.9373
43	*Argania Spinosa*	0.8509	93	*Kappaphycus alvarezi*	0.3493
44	*Saccharum officinarum*	0.9545	94	*Dimocarpus longan*	0.2267
45	*Cassia* sp.	0.9255	95	*Hordeum vulgare*	0.9117
46	*Aleurites moluccanus*	0.8471	96	*Arachis hypogaea*	0.0464
47	*Prunus dulcis*	0.7297	97	*Castanea crenata*	0.3165
48	*Manilkara bidentata*	0.3356			
49	*Vigna aconitifolia*	0.9796			
50	*Abelmoschus esculentus*	0.8246			

Right panel shows levels of ANGPTL2 protein in the medium relative to control untreated cells. Data from untreated control HPAC cells were set to 1. Gray shading indicates values <0.4 relative to control.

Angptl2-overexpressing cells increased relative to those from mock-transfected control cells (Figure 1J,K). We conclude that ANGPTL2 upregulation in keratinocytes increases secretion of factors known to regulate tyrosinase expression in neighbouring melanocytes.

3.3 | An extract from *Chrysanthemum indicum* × *Erigeron annuus* antagonizes ANGPTL2 expression in a cell culture model

We next asked whether traditional Chinese medicines derived from natural products might inhibit ANGPTL2 expression. For this analysis, we chose the human pancreatic cancer line HPAC, as it expresses high levels of ANGPTL2. We treated HPAC cells with one of 97 products shown in Table 1 and measured ANGPTL2 protein levels in culture media 24 hours later using ELISA. Among them, 20 products inhibited ANGPTL2 expression, and we focused on product #84, a water extract of a product derived from *Chrysanthemum indicum* × *Erigeron annuus* (CE) (Table 1). Subsequently, we found that CE extracted in either water (#84) or alcohol (#85) (see Table 1) was equally effective in inhibiting ANGPTL2 expression in HPACs. Therefore, to minimize toxicity, we chose the water-extracted product #84 (CE) for further analysis. Further toxicity analysis conducted in B16 cells revealed no change in viability in CE-treated vs untreated cells, even at concentrations as high as high (1.0 mg/mL) (Figure 2A).

3.4 | CE treatment of melanoma cells suppresses IBMX-dependent melanin production and tyrosinase expression

Treatment of melanocytes with the compound 3-isobutyl-1-methylxanthine (IBMX) increases intracellular cAMP levels and, like UV-B exposure, promotes melanin production.[20] Given that UV-B directly induces *Angptl2* mRNA in B16 melanoma cells (Figure 1A), we asked whether IBMX treatment would alter ANGPTL expression in B16 cells. Treatment of B16 cells with IBMX alone increased ANGPTL2 protein levels secreted in the media relative to untreated controls (Figure 2B). We had previously reported that NFATc2 is required for *Angptl2* expression in lung cancer cells.[9] When we asked whether IBMX treatment induced NFATc2 in B16 cells, we observed that IBMX treatment induced levels of intracellular NFATc2 protein to levels greater than those seen in controls (Figure 2C). However, ANGPTL2 protein levels were comparable and relatively low in both control and IBMX-treated cells in the presence of CE (Figure 2B). We next asked whether CE treatment blocks melanin production in IBMX-treated melanoma cells. Treatment with IBMX increased intracellular melanin content of B16 cells, based on ELISA and this effect was blocked by co-treatment with CE (Figure 2D). Cells not treated with IBMX showed comparable melanin production in the presence or absence of CE (Figure 2D). Treatment of B16 cells with IBMX also increased tyrosinase activity and *Tyr* transcript levels, and both of these outcomes were blocked in the presence of CE (Figure 2E,F). B16 cells not treated with IBMX showed comparable tyrosinase activity and *Tyr* mRNA induction in the presence or absence of CE (Figure 2E,F). We then asked whether CE directly decreases tyrosinase activity by performing in vitro assays of mushroom tyrosinase activity. Interestingly, CE treatment did not alter tyrosinase activity (Figure 2G), suggesting that CE antagonizes tyrosinase expression rather than activity.

IBMX reportedly stimulates expression of melanogenic genes, including MITF, via a cAMP-dependent pathway.[2,21] Therefore, we next asked whether CE affects IBMX-induced melanogenesis independent of ANGPTL2. To do so, we first generated *Angptl2* knockdown B16 cells with siRNA and confirmed that *Angptl2* expression decreased in those cells relative to B16 cells transduced with scrambled control siRNA (Figure 2H). We then examined whether expression of melanogenic genes was upregulated in IBMX-treated *Angptl2* knockdown cells and observed increases in *Tyrosinase*, *Mitf*, *Trp1* and *Trp2* mRNAs in those cells relative to *Angptl2* knockdown cells not treated with IBMX (Figure 2I-L). However, induction of these mRNAs was significantly repressed

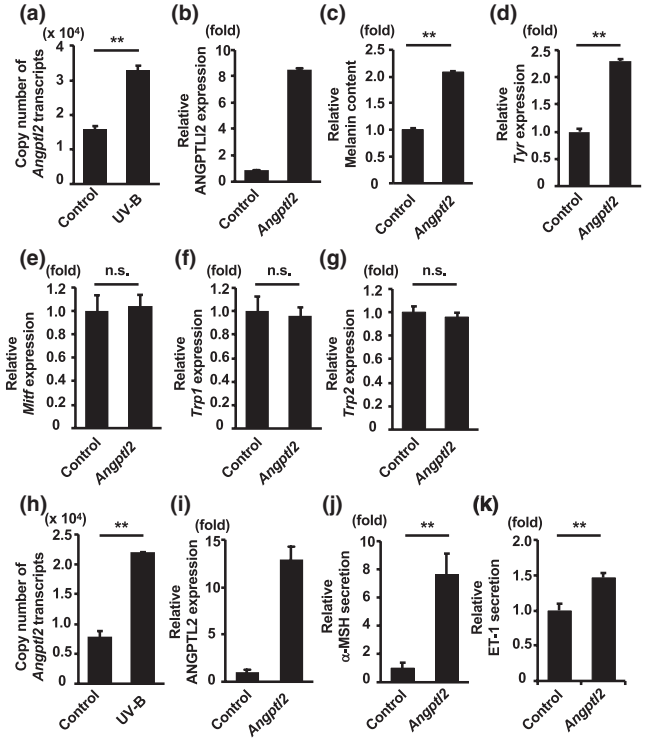

FIGURE 1 Angiopoietin-like protein 2 (ANGPTL2) expression induces factors required for melanin synthesis in melanocytes and keratinocytes. Copy number of *Angptl2* cDNA per μl after real-time RT-PCR in B16 cells with (n = 3) or without (n = 3) UV-B irradiation (A). Relative ANGPTL2 protein levels in culture medium of *Angptl2*-overexpressing (*Angptl2*) (n = 2) vs Control (n = 2) B16 cells. Results in B are shown as means ± ranges (B). Relative melanin protein content in *Angptl2*-overexpressing (*Angptl2*) (n = 3) vs Control (n = 3) B16 cells (C). Relative expression of *Tyr* mRNA in *Angptl2*-overexpressing (n = 3) and vs Control (n = 3) B16 cells (D). Relative expression of *Mitf* (E), *Trp1* (F) *and Trp2* (G) mRNAs in *Angptl2*-overexpressing (n = 3) and vs Control (n = 3) B16 cells. Copy number of *Angptl2* cDNA per μl after real-time RT-PCR of HaCaT cells with (n = 3) or without (n = 3) UV-B irradiation (H). Relative ANGPTL2 protein levels in culture medium of *Angptl2*-overexpressing (n = 2) vs Control (n = 2) HaCaT cells. Results in I are means ± ranges (I). Relative α-MSH protein levels in culture media from *Angptl2*-overexpressing (n = 4) and Control (n = 4) HaCaT cells (J). Relative ET-1 protein levels in culture media from *Angptl2*-overexpressing (n = 4) vs Control (n = 4) HaCaT cells (K). Data from controls was set to 1. Error bars show SEM (A, C, D, E, F, G, I, J and K). $^{**}P < 0.01$, Student's *t* test

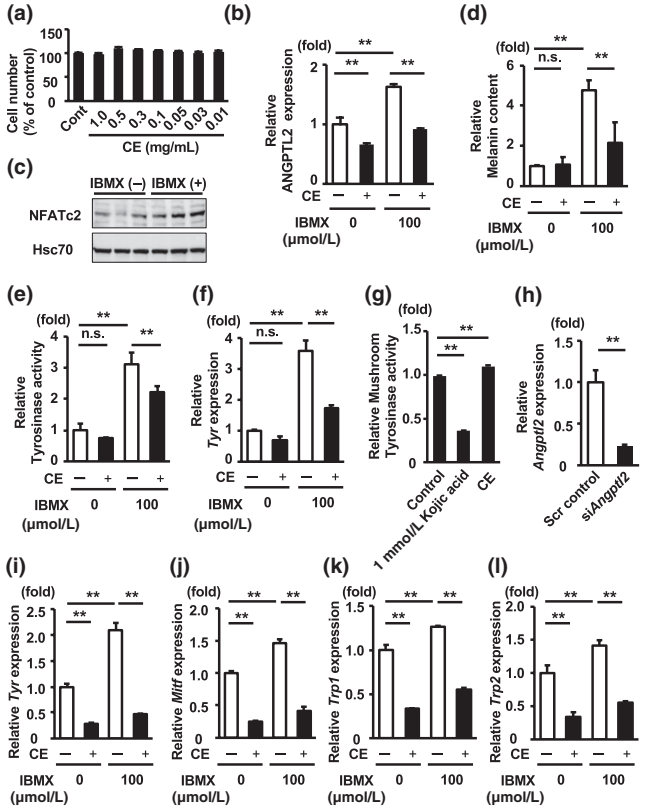

FIGURE 2 Extract from *Chrysanthemum indicum* × *Erigeron annuus* suppresses ANGPTL2 expression. Viability of B16 cells treated with various CE concentrations (n = 3). Data from control cells were set to 100. Error bars show SEM (A). Relative expression of ANGPTL2 protein in the medium in IBMX-treated B16 cells with (n = 4) or without (n = 4) CE treatment (B). Representative image of immunoblotting analysis for NFATc2 protein in B16 cells with or without IBMX treatment (100 μM). Hsc70 served as a loading control (C). Relative melanin protein content in IBMX-treated B16 cells with (n = 4) or without (n = 4) CE treatment (D). Relative tyrosinase activity in IBMX-treated B16 cells with (n = 4) or without (n = 4) CE treatment (E). Relative expression of *Tyr* mRNA in IBMX-treated B16 cells with (n = 3) or without (n = 3) CE treatment (F). Data from control cells not treated with either IBMX or CE (0.5 mg/mL) was set to 1. Error bars show SEM from three (B, D, E and F) different experiments. $^{**}P < 0.01$, n.s., not statistically significant by Student's *t* test. Relative mushroom tyrosinase activity in vitro with (n = 4) or without (n = 4) CE (0.5 mg/mL) treatment (G). Kojic acid, which inhibits mushroom tyrosinase activity, served as a positive control. Control value was set to 1. Error bars show SEM (G). Data from B16 cells treated without both IBMX and CE were set to 1. $^{**}P < 0.01$ by Student's *t* test. Relative expression of *Angptl2* mRNA in B16 cells treated with scrambled control (Scr control) (n = 3) or *Angptl2* (si*Angptl2*) (n = 3) siRNA. H, Data from control cells treated with scrambled control *siRNA* were set to 1. Relative expression of *Tyr* (I), *Mitf* (J), *Trp1* (K) and *Trp2* (L) mRNAs in *Angptl2* knockdown B16 cells (n = 3) either untreated or treated with IBMX and CE, either alone or in combination. Data from B16 cells not treated with either were set to 1. $^{**}P < 0.01$ by Student's *t* test

in *Angptl2* knockdown B16 cells that were either treated or not treated with IBMX in the presence of CE (Figure 2I-L). We conclude that CE represses IBMX-induced melanogenesis independent of ANGPTL2 activity.

3.5 | CE treatment suppresses α-MSH and ET-1 expression in keratinocytes

Next, we examined the effect of CE on the keratinocyte line HaCaT. Treatment of HaCaT cells with UV-B increased *Angptl2* mRNA levels, and those levels decreased relative to untreated control cells when irradiated cells were treated with CE immediately after irradiation (Figure 3A). In addition, treatment of HaCaT cells with UV-B increased *Edn1* (which encodes ET-1) and *Pomc*

(which encodes α-MSH) transcript levels, while treatment of irradiated cells with CE immediately after irradiation decreased those values (Figure 3B,C). As noted, NFATc2 is required for *Angptl2* expression.[9] Here, we found that treatment of B16 cells with IBMX increased intracellular NFATc2 protein levels (Figure 2C). Mechanistically, IBMX upregulates cAMP signalling, which induces NFAT activities.[2,21–23] UV-B also reportedly induces NFATs in T cells.[24] Therefore, we asked whether UV-B directly induces NFATc2 in HaCaT or B16 cells. In both, UV-B treatment induced intracellular NFATc2 protein to levels greater than those seen in corresponding controls (Figure 3D,E). However, irradiated HaCaT or B16 cells treated with CE showed NFATc2 levels comparable to corresponding untreated controls (Figure 3D,E), suggesting that CE inhibition of *Angptl2* induction does not require changes in NFATc2 expression. These mechanisms should be examined in future studies.

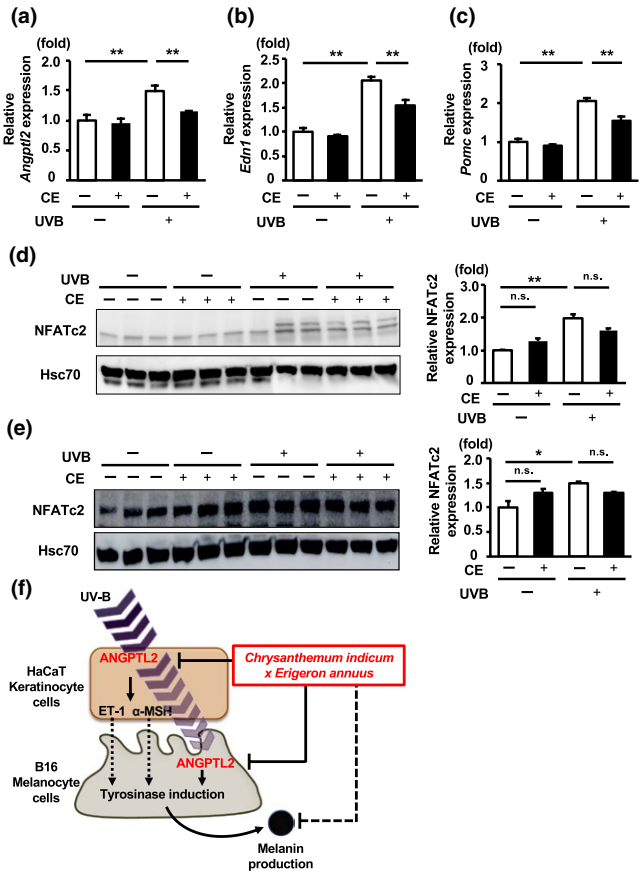

FIGURE 3 CE suppresses α-MSH and ET-1 expression in keratinocytes. Relative expression of *Angptl2* mRNAs in UV-B-exposed HaCaT cells, with (n = 3) or without (n = 3) CE treatment (A). Relative expression of *Edn1* mRNA, which encodes ET-1, in UV-B-exposed HaCaT cells, with (n = 3) or without (n = 3) CE treatment (B). Relative expression of *Pomc* mRNA, which encodes α-MSH, in UV-B-exposed HaCaT cells, with (n = 3) or without (n = 3) CE treatment. (C). Representative image showing immunoblotting for NFATc2 protein in UV-B-exposed HaCaT cells treated with or without CE (0.5 mg/mL). Hsc70 served as a loading control (D: left panel). Relative expression of NFATc2 protein in UV-B-exposed HaCaT cells, treated with or without CE (0.5 mg/mL) (n = 3, respectively) (D: right panel). Representative image of immunoblotting for NFATc2 protein in UV-B-exposed B16 cells treated with or without CE (0.5 mg/mL). Hsc70 served as a loading control (E: left panel). Relative expression of NFATc2 protein in UV-B-exposed B16 cells treated with or without CE (0.5 mg/mL) (n = 3, respectively) (E: right panel). Values from control HaCaT or B16 cells not treated with either UV-B or CE (0.5 mg/mL) were set to 1. Error bars show SEM (A, B, C, D and E). **P* < 0.05, ***P* < 0.01 by Student's *t* test. Schema showing melanin production promoted by ANGPTL2 and suppressed by CE (F)

4 | DISCUSSION

In this study, using cultured keratinocytes and melanoma cells as models, we provide evidence suggesting that UV-B radiation accelerates melanin production and accumulation in skin tissue by inducing ANGPTL2 expression in two cell types. We also found that the natural product compound CE inhibits ANGPTL2 production in both keratinocytes and melanoma cells, as illustrated in the model shown in Figure 3F. CE inhibited ANGPTL2 expression in melanocytes with little toxicity or change in cell viability. In addition, CE repressed IBMX-induced melanogenesis independent of ANGPTL2 activity. We conclude that CE could serve as a relatively non-toxic component of whitening cosmetics, as it blocks melanin accumulation associated with hyperpigmentation and appearance of spots and freckles.[25]

ET-1 and α-MSH secreted by keratinocytes are important mediators of melanin production[18,19] and are induced by inflammatory cytokines via NF-κB signalling.[18,26,27] We previously reported that ANGPTL2 activates NF-κB signalling in endothelial cells in an autocrine manner.[10] Therefore, ANGPTL2 expression in keratinocytes may induce ET-1 and α-MSH through NF-κB signalling.

Tyrosinase activity in melanocytes is required for melanin production.[28] Here, we showed that ANGPTL2 expression in melanoma cells increased tyrosinase mRNA levels rather than catalytic activity of tyrosinase protein. STAT3 reportedly induces tyrosinase expression in melanocytes.[29] We previously reported that ANGPTL2 induces IL-6 in endothelial cells and macrophages, which activate STAT3 signalling.[30,31] Therefore, tyrosinase induction by ANGPTL2 in melanoma cells might be due to upregulated IL-6 and STAT3 activity.

CE is derived from an asteraceae plant cultivated in a region of Shiranui town in the Kumamoto prefecture in Japan. When extracted in water or alcohol, it has been used as a traditional herbal medicine to maintain overall good health. Interestingly, CE extracts made from plant petals reportedly suppress proliferation of various cancer lines.[32] Moreover, relevant to immune responses, CE extracts suppress histamine release from the basophil cell line RBL-2H3.[33] Mechanisms underlying these effects are unknown, but based on our findings, future analysis should address whether any of these outcomes are due to ANGPTL2 inhibition. NFATc2 is reportedly required for *Angptl2* expression[9]; however, we found that CE extracts inhibit ANGPTL2 but not via NFATc2 inhibition.

Therefore, we undertook analysis of the *Angptl2* promoter using the UCSC genome browser and observed binding motifs for many transcription factors that may potentially regulate *Angptl2*. Among them is USF1, a transcription factor induced by UV-B,[34,35] as well as the cAMP response element binding protein (CREB).[36] We conclude that CE extracts may inhibit ANGPTL2 by intefering with USF1 transcriptional activity, a mechanism we will explore in future studies.

Melanin is the first line of defence against DNA damage at the skin surface.[37] Therefore, total inhibition of melanin production could leave skin vulnerable to DNA damage. On the other hand, excess ANGPTL2 expression in skin tissue is inflammatory and associated with carcinogenesis.[11,38] Therefore, future studies should examine mechanisms governing potentially inflammatory ANGPTL2 activity in skin.

ACKNOWLEDGEMENTS

We thank Mr. Hiroshi Oshiumi and Mr. Takumi Kido for technical assistance.

CONFLICT OF INTEREST

GS, DM and TI are employees of Saishunkan Pharmaceutical Co., Ltd. YO has received a research grant from Saishunkan Pharmaceutical Co., Ltd. ME has no conflicts of interest.

AUTHOR CONTRIBUTIONS

GS, ME, DM, TI and YO contributed to the conception and design of the study. GS and ME performed the research. GS and ME wrote the manuscript. All authors read the manuscript and approved its submission.

ORCID

Motoyoshi Endo https://orcid.org/0000-0002-8287-2456

REFERENCES

[1] N. Silpa-Archa, I. Kohli, S. Chaowattanapanit, H. W. Lim, I. Hamzavi, *J. Am. Acad. Dermatol.* **2017**, *77*, 591.
[2] Y. Yamaguchi, V. Hearing, *BioFactors* **2009**, *35*, 193.
[3] H. Park, M. Kosmadaki, M. Yaar, B. A. Gilchrest, *Cell. Mol. Life Sci.* **2009**, *66*, 1493.
[4] Y. Ochiai, K. Torii, Y. Okano, H. Masaki, *J. Soc. Cosmet. Chem. Jpn.* **2000**, *34*, 47.
[5] T. Kadomatsu, M. Endo, K. Miyata, Y. Oike, *Trends Endocrinol. Metab.* **2014**, *25*, 245.
[6] Y. Oike, Z. Tian, K. Miyata, J. Morinaga, M. Endo, T. Kadomatsu, *Circ. J.* **2017**, *81*, 1379.
[7] Z. Tian, K. Miyata, T. Kadomatsu, H. Horiguchi, H. Fukushima, S. Tohyama, Y. Ujihara, T. Okumura, S. Yamaguchi, J. Zhao, M. Endo, J. Morinaga, M. Sato, T. Sugizaki, S. Zhu, K. Terada, H. Sakaguchi, Y. Komohara, M. Takeya, N. Takeda, K. Araki, I. Manabe, K. Fukuda, K. Otsu, J. Wada, T. Murohara, S. Mohri, J. K. Yamashita, M. Sano, Y. Oike, *Nat. Commun.* **2016**, *7*, 13016.
[8] M. Endo, Y. Yamamoto, M. Nakano, T. Masuda, H. Odagiri, H. Horiguchi, K. Miyata, T. Kadomatsu, I. Motokawa, S. Okada, H. Iwase, Y. Oike, *Int. J. Biol. Markers* **2014**, *29*, 5000080.
[9] M. Endo, M. Nakano, T. Kadomatsu, S. Fukuhara, H. Kuroda, S. Mikami, T. Hato, J. Aoi, H. Horiguchi, K. Miyata, H. Odagiri, T. Masuda, M. Harada, H. Horio, T. Hishima, H. Nomori, T. Ito, Y. Yamamoto, T. Minami, S. Okada, T. Takahashi, N. Mochizuki, H. Iwase, Y. Oike, *Cancer Res.* **2012**, *72*, 1784.
[10] M. Tabata, T. Kadomatsu, S. Fukuhara, K. Miyata, Y. Ito, M. Endo, T. Urano, H. J. Zhu, H. Tsukano, H. Tazume, K. Kaikita, K. Miyashita, T. Iwawaki, M. Shimabukuro, K. Sakaguchi, T. Ito, N. Nakagata, T. Yamada, H. Katagiri, M. Kasuga, Y. Ando, H. Ogawa, N. Mochizuki, H. Itoh, T. Suda, Y. Oike, *Cell Metab.* **2009**, *10*, 178.
[11] J. Aoi, M. Endo, T. Kadomatsu, K. Miyata, M. Nakano, H. Horiguchi, A. Ogata, H. Odagiri, M. Yano, K. Araki, M. Jinnin, T. Ito, S. Hirakawa, H. Ihn, Y. Oike, *Cancer Res.* **2011**, *71*, 7502.
[12] L. Chen, W. Chang, C. Lee, L. T. Lee, C. M. Shih, C. C. Wang, *Biol. Pharm. Bull.* **2009**, *32*, 1447.
[13] R. Lam, Z. Lin, E. Sviderskaya, C. H. Cheng, *J. Ethnopharmacol.* **2010**, *132*, 274.
[14] B. Wu, *Curr. Top. Med. Chem.* **2014**, *14*, 1425.
[15] T. Lei, V. Virador, W. Vieira, V. J. Hearing, *Anal. Biochem.* **2002**, *305*, 260.
[16] K. Kim, J. Kim, S. Eom, S. H. Lee, K. R. Min, Y. Kim, *Pigment Cell Res.* **2006**, *19*, 90.
[17] J. Yang, J. Koo, Y. Song, K. B. Kwon, J. H. Lee, H. S. Sohn, B. H. Park, E. C. Jhee, J. W. Park, *Acta Pharmacol. Sin.* **2006**, *27*, 1467.
[18] G. Imokawa, Y. Yada, M. Miyagishi, *J. Biol. Chem.* **1992**, *267*, 24675.
[19] A. Chakraborty, Y. Funasaka, A. Slominski, G. Ermak, J. Hwang, J. M. Pawelek, M. Ichihashi, *Biochim. Biophys. Acta* **1996**, *1313*, 130.
[20] T. Hoshino, M. Matsuda, Y. Yamashita, M. Takehara, M. Fukuya, K. Mineda, D. Maji, H. Ihn, H. Adachi, G. Sobue, Y. Funasaka, T. Mizushima, *J. Biol. Chem.* **2010**, *285*, 13254.
[21] R. Busca, R. Ballotti, *Pigment Cell Res.* **2000**, *13*, 60.
[22] M. Schmidt, F. Dekker, H. Maarsingh, *Pharmacol. Rev.* **2013**, *65*, 670.
[23] S. Giampaolo, G. Wojcik, S. Klein-Hessling, E. Serfling, A. K. Patra, *Oncotarget* **2017**, *9*, 9632.
[24] C. Huang, P. Mattjus, W. F. Ma, M. Rincon, N. Y. Chen, R. E. Brown, Z. Dong, *J. Biol. Chem.* **2000**, *275*, 9143.
[25] S. Chou, W. Chang, C. Chang, S. L. Hsu, Y. C. Lin, Y. Shih, *Int. J. Mol. Sci.* **2013**, *14*, 19186.
[26] T. Brzoska, D. Kalden, T. Scholzen, T. A. Luger, *Ann. N. Y. Acad. Sci.* **1999**, *885*, 230.
[27] S. Manna, B. Aggarwal, *J. Immunol.* **1998**, *161*, 2873.
[28] S. D' Mello, G. Finlay, B. Baguley, M. E. Askarian-Amiri, *Int. J. Mol. Sci.* **2016**, *17*, 1144.
[29] C. Yang, M. Fan, A. Slominski, J. Yue, L. M. Pfeffer, *Int. J. Interferon Cytokine Mediat. Res.* **2010**, *2010*, 1.
[30] E. Horio, T. Kadomatsu, K. Miyata, Y. Arai, K. Hosokawa, Y. Doi, T. Ninomiya, H. Horiguchi, M. Endo, M. Tabata, H. Tazume, Z. Tian, O. Takahashi, K. Terada, M. Takeya, H. Hao, N. Hirose, T. Minami, T. Suda, Y. Kiyohara, H. Ogawa, K. Kaikita, Y. Oike, *Arterioscler. Thromb. Vasc. Biol.* **2014**, *34*, 790.
[31] M. Yugami, H. Odagiri, M. Endo, H. Tsutsuki, S. Fujii, T. Kadomatsu, T. Masuda, K. Miyata, K. Terada, H. Tanoue, H. Ito, J. Morinaga, H. Horiguchi, T. Sugizaki, T. Akaike, T. Gotoh, T. Takai, T. Sawa, H. Mizuta, Y. Oike, *J. Biol. Chem.* **2016**, *291*, 18843.
[32] K. Murayama, T. Sawa, H. Koga, S. Yamaguchi, M. Kumazoe, T. Otsuka, Y. Miyazaki, H. Tachibana, K. Yamada, *Nippon Shokuhin Kagaku Kogaku Kaishi* **2013**, *60*, 80.
[33] K. Yamada, T. Sawa, K. Murayama, S. Yamaguchi, Y. Miyazaki, H. Tachibana, *Nippon Shokuhin Kagaku Kogaku Kaishi* **2012**, *59*, 394.
[34] S. Corre, A. Primot, E. Sviderskaya, D. C. Bennett, S. Vaulont, C. R. Goding, M. D. Galibert, *J. Biol. Chem.* **2004**, *279*, 51226.

[35] A. Bouafia, S. Corre, D. Gilot, N. Mouchet, S. Prince, M. D. Galibert, *PLoS Genet*. **2014**, *10*, e1004309.
[36] J. Steiger, S. Bandyopadhyay, D. Farb, S. J. Russek, *J. Neurosci.* **2004**, *24*, 6115.
[37] A. Godic, B. Poljsak, M. Adamic, R. Dahmane, *Oxid. Med. Cell Longev.* **2014**, *2014*, 1.
[38] J. Aoi, M. Endo, T. Kadomatsu, K. Miyata, A. Ogata, H. Horiguchi, H. Odagiri, T. Masuda, S. Fukushima, M. Jinnin, S. Hirakawa, T. Sawa, T. Akaike, H. Ihn, Y. Oike, *Mol. Cancer Res*. **2014**, *12*, 239.

How to cite this article: Satou G, Maji D, Isamoto T, Oike Y, Endo M. UV-B-activated B16 melanoma cells or HaCaT keratinocytes accelerate signaling pathways associated with melanogenesis via ANGPTL 2 induction, an activity antagonized by Chrysanthemum extract. *Exp Dermatol*. 2019;28:152–160. https://doi.org/10.1111/exd.13862